Performance Improvement of Glass Fiber–Poly(phenylene sulfide) Composite

JYONGSIK JANG* and HAK SUNG KIM

Department of Chemical Technology, College of Engineering, Seoul National University, San 56-1, Shinlimdong Kwanakgu, Seoul, Korea

SYNOPSIS

In order to improve the mechanical properties of glass fiber–poly(phenylene sulfide) (GF–PPS) composite, silane coupling agents were used to modify the glass fiber surface. RC-2 silane and styryl silane were applied to the surface treatment of glass fiber with various concentrations. The interlaminar shear strength and the flexural strength of the silane treated GF–PPS composite increased compared with the untreated one. The optimum silane concentrations for the glass surface treatment were observed in RC-2 silane and styryl silane, respectively. RC-2 silane was more effective in the enhancement of the interlaminar shear strength and the flexural strength of the GF–PPS composite. © 1996 John Wiley & Sons, Inc.

INTRODUCTION

Fiber-reinforced polymer composite has been widely used as high performance material in aerospace and automotive applications.[1-3] Recently, a thermoplastic polymer composite has been developed for general purpose and specialty fields. When the thermoplastic is used for the matrix resin, easy processibility and recyclability of the polymer composite can be obtained.[4] Major thermoplastics as matrices for high performance polymer composite are poly(phenylene sulfide) (PPS), poly(butylene terephthalate) (PBT), poly(ether ether ketone) (PEEK), and so forth.

PPS is a crystalline engineering plastic and has excellent physical, chemical, and mechanical properties. When PPS is reinforced with glass fiber, higher mechanical strength and lower cost can be obtained compared with the case of PPS only. Therefore, most PPS is supplied as a compound with glass fiber.[5-11] PPS is generally considered as a thermoplastic but possesses some thermoset characters. When it is heated in air at a temperature above its melting point, a cross-linking reaction can take place.[12]

The interfacial adhesion between fiber and matrix

has been known as an important factor that determines the mechanical strength of the polymer composite, and it becomes more important under hot/wet conditions.[13] In general, the thermoplastic polymer composite has poor adhesion at the interface between fiber and matrix. To improve the interfacial adhesion, various techniques of fiber surface treatment have been studied.[14-17] Silane coupling agents have been well known as adhesion promoters of the polymer composite interface. Many studies have reported that the mechanical properties of the polymer composite were increased by silane coupling agents.[18-23]

When silane coupling agents are introduced onto the glass fiber surface in the composite, two interfaces exist between glass fiber and polymer matrix: (1) the interface between glass fiber and silane coupling agents, and (2) the interface between silane coupling agents and polymer matrix.

At the interface between the glass fiber and the silane coupling agent, the hydroxyl groups of the silanes and those of the glass fiber surface can react with each other through siloxane bonding or hydrogen bonding. Interfacial adhesion can be promoted by this mechanism.[13] Figure 1 indicates the adsorption process of the silane coupling agents onto the glass surface.
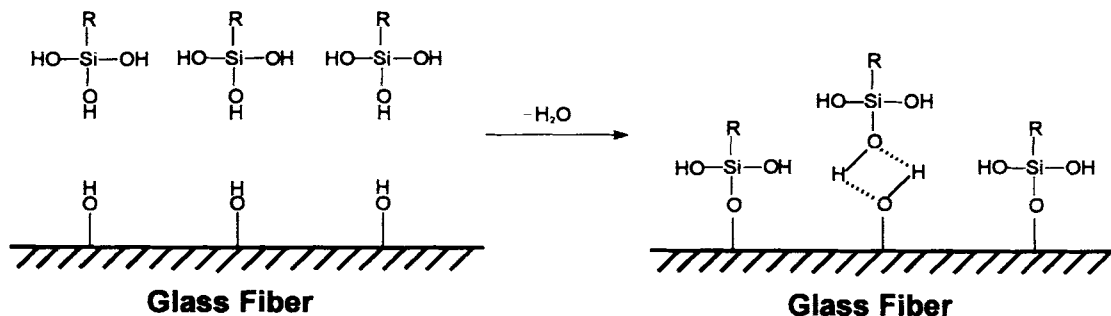

Figure 1   The adsorption process of the silane coupling agents onto the glass surface.

At the interface between the silane coupling agents and polymer matrix, three representative mechanisms of the adhesion promotion have been suggested. First, silane coupling agents react chemically with the polymer matrix at the molding temperature, and the interfacial adhesion can be strengthened. Interpenetrating polymer network (IPN) theory is regarded as another mechanism of adhesion promotion. An IPN is formed through the interdiffusion of the polymer matrix and silane in the interphase region. At high temperature in the composite manufacturing process, the silane coupling agents on the glass surface diffuse into the polymer matrix phase and act as a partial solvent of the polymer matrix in the vicinity of the glass fiber surface. However, as the composite cools, the polymer loses its solubility and separates as an interpenetrating phase with the siloxane at the inter-
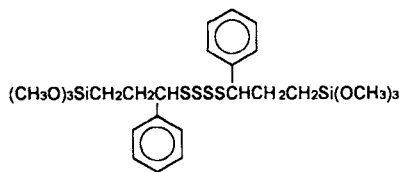
phase of the composite. Finally, the compatibility of the silane coupling agents with the polymer matrix is a factor in determining the interfacial adhesion strength between the silane and the polymer matrix.[24]

The purpose of this paper was to investigate the surface modification of glass fiber using silane coupling agents. The mechanical properties of the GF–PPS composite were also evaluated under the different surface treatment conditions, and morphological studies of fracture surfaces of the GF–PPS composites were carried out. In addition, the relationship between the surface treatment of the glass fiber and the mechanical properties of the composite was also studied.

EXPERIMENTAL

PPS (Suntra S 500) was supplied in the form of powder from Sunkyung Industry Co., and glass fab-

a) RC-2 silane

$(CH_3O)_3SiCH_2CH_2CHSSSSCHCH_2CH_2Si(OCH_3)_3$

b) Styryl silane

$CH_2=CH-\langle O \rangle-CH_2NH_2CH_2CH_2CH_2NH\ CH_2CH_2CH_2Si(OCH_3)_3$ $^\ominus Cl$
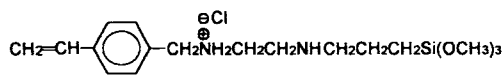
Figure 2   The structure of silane coupling agents.
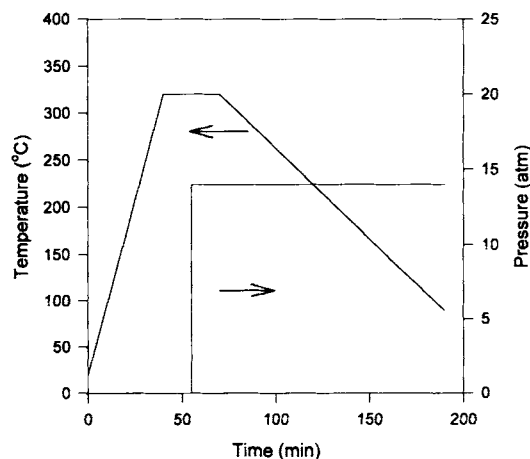

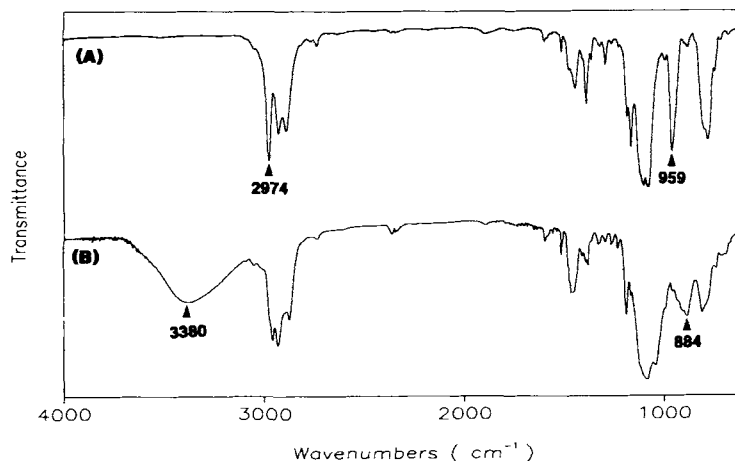**Figure 3**   Composite manufacturing cycle.

Figure 4   Transmission spectra of RC-2 silane (A) before hydrolysis and (B) after hydrolysis.

ric (H-118) was purchased in the preheated state from Hankook Fiber Co. Tables I and II show the basic properties of PPS and glass fiber, respectively. The glass fiber was dried at 200°C for 16 h to remove water on the glass surface. To improve the interfacial adhesion of GF–PPS composite, UCARSIL™ RC-2 silane (RC-2 silane) and 3-(N-styrylmethyl-2-amino-ethylamino)-propyltrimethoxy silane hydro chloride (styryl silane) were introduced. RC-2 silane was purchased from Union Carbide Co. and styryl silane from Dow Corning Co. The structures of the silane coupling agents used in this experiment are given in Figure 2.

In order to treat glass surface under various conditions, five kinds of silane solutions for each silane coupling agent were prepared. In those solutions, cosolvent of n-butyl alcohol (95 wt % in total solvent) and distilled water (5 wt % in total solvent) was used, and the silane concentration was varied from 0.1 to 0.5 wt % in total solvent. After the silane coupling agents were hydrolyzed at pH 3.5 for 1 h, the glass fiber was dipped in the hydrolyzed silane solution for 10 min, and it was dried at room temperature for 48 h.

A Fourier transform–infrared (FTIR) spectrophotometer (BOMEM MB 100) was used with a
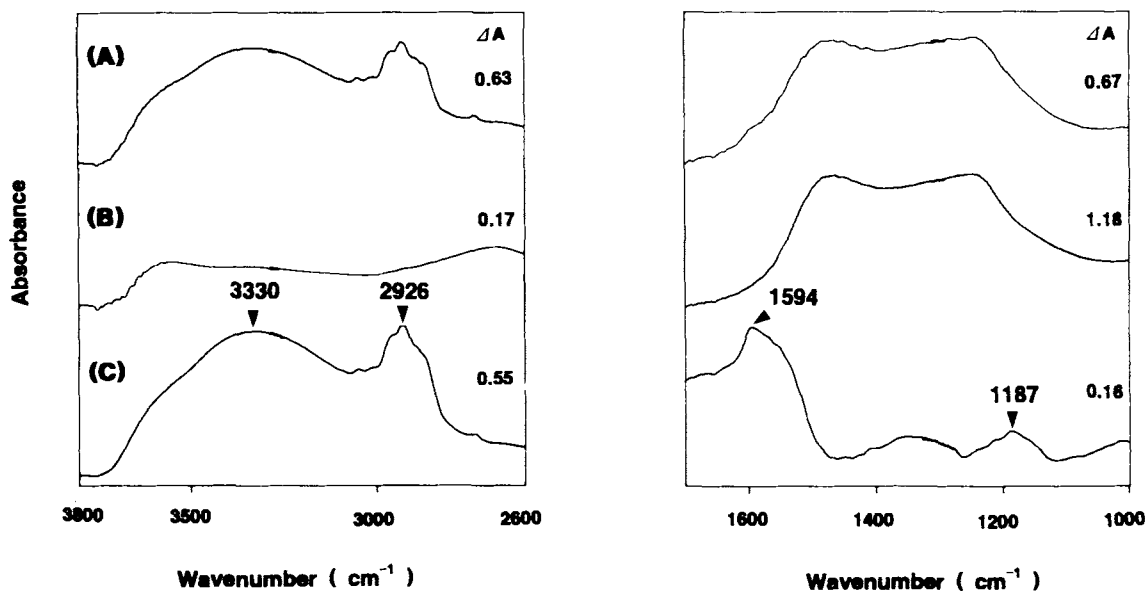

Figure 5   DRIFT spectra of RC-2 silane-treated glass fiber. (A) RC-2 silane treated glass fiber. (B) Glass fiber. (C) Difference spectrum: (A) − (B).

Transmittance

(A)

3337　2832

1193

1030

(B)

3421

1561

908

4000　3000　2000　1000
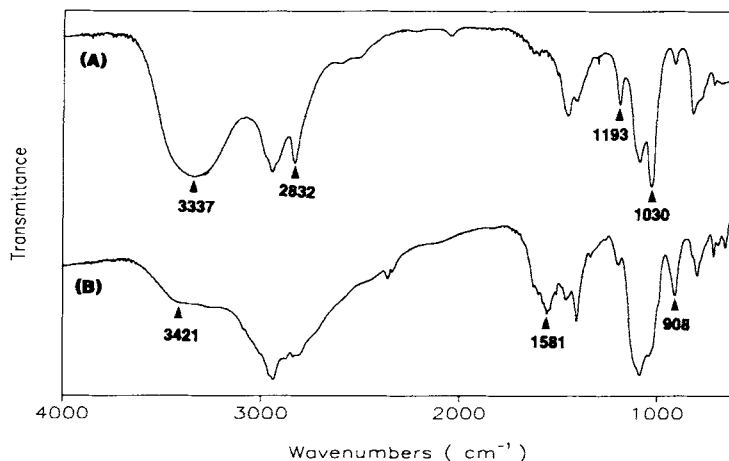
Wavenumbers (cm⁻¹)

Figure 6 Transmission spectra of styryl silane (A) before hydrolysis and (B) after hydrolysis.

deuterated triglycin sulfate detector at a resolution of 4 cm⁻¹. The spectrophotometer was purged with dry nitrogen to reduce the concentration of atmospheric water vapor and carbon dioxide.

It was intended to compare the spectra of silane coupling agents before hydrolysis with those after hydrolysis. For that purpose, the RC-2 silane and the styryl silane samples were prepared as follows. After the RC-2 silane and the styryl silane at 10 wt % concentration were hydrolyzed in n-butyl alcohol/water (97/3 wt %), one drop of the solution was cast on the potassium bromide pellet and dried at room temperature. Each spectrum was recorded with 20 scans.

Diffuse reflectance technique (DRIFT) was used for the identification of silane coupling agents adsorbed onto the glass fiber surface. For the spectra, 200 scans were coadded.

To manufacture the GF–PPS composite, compression mold was used in this experiment. The glass fabrics of 16 layers and PPS powder were stacked alternately in the mold. The composite was fabricated by heating to 320°C, pressing at 14 atm and then cooling at a rate of 2°C/min room temperature. Figure 3 shows the temperature and pressure profile of the composite manufacturing.

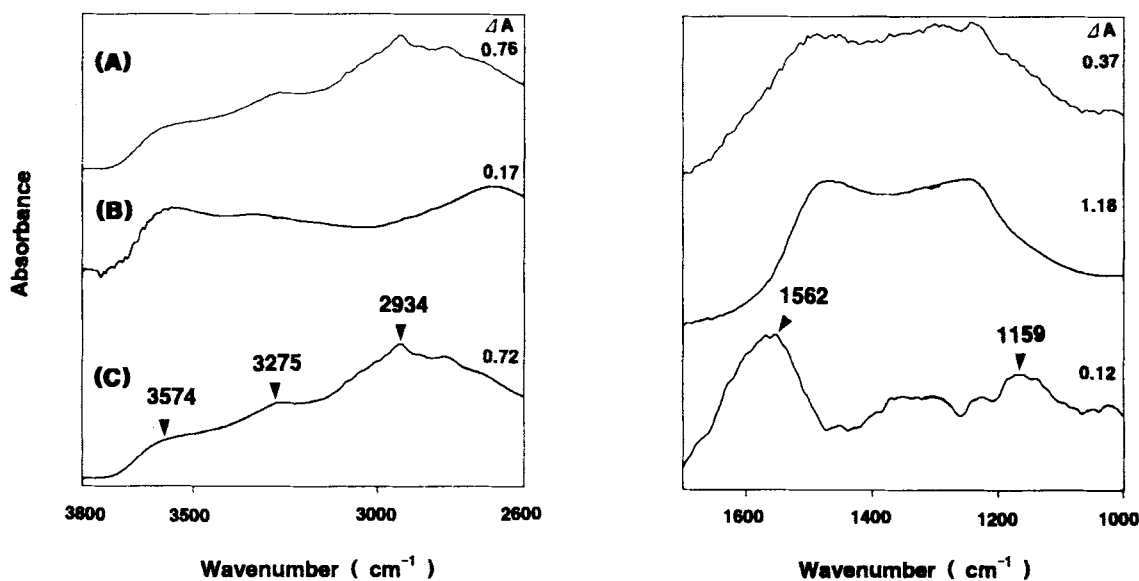To estimate the interfacial adhesion strength of

Absorbance

(A)　△A 0.76

(B)　0.17

(C)　2934　0.72
3574　3275

3800　3500　3000　2600

Wavenumber (cm⁻¹)

△A 0.37

1.18

1562

1159　0.12

1600　1400　1200　1000

Wavenumber (cm⁻¹)

Figure 7 DRIFT spectra of styryl silane-treated glass fiber. (A) Styryl silane treated glass fiber. (B) Glass fiber. (C) Difference spectrum: (A) − (B).
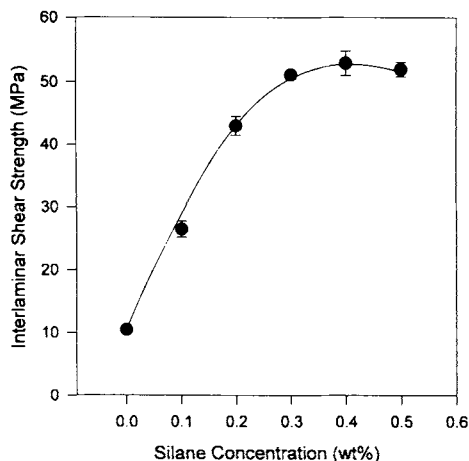
Figure 8 Interlaminar shear strength of RC-2 silane treated GF–PPS composite.

Figure 10 Interlaminar shear strength of styryl silane treated GF–PPS composite.

the composite, the measurement of the interlaminar shear strength was performed according to ASTM D 2344. Specimens of 2 × 10 × 14 mm³ were used for interlaminar shear strength test. The span length was 10 mm, and the crosshead speed was 1.3 mm/min. At least five tests were averaged.

The measurement of the flexural strength was performed according to ASTM D 790. Three point bend specimens of 2 × 10 × 42 mm³ were used for the flexural strength test. The span length was 32 mm, and the crosshead speed was 2.0 mm/min. At least five tests were averaged as in the case of ILSS.

A JEOL scanning electron microscope (JSM-35) was used to analyze the fracture surfaces of the GF–PPS composites. All specimens were coated with a
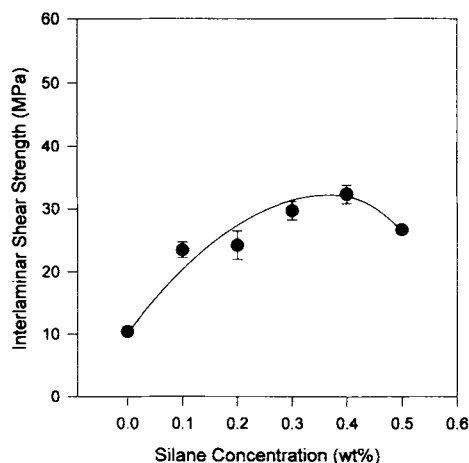
thin layer of gold to eliminate charging effects. A 1500 magnification was utilized in the SEM examination.

RESULTS AND DISCUSSION

A FT-IR spectrophotometer was applied to observe the silane coupling agents adsorbed on the glass fiber surface after hydrolysis. The FT-IR transmittance spectra of RC-2 silane before and after hydrolysis are shown in Figure 4. The spectrum of pristine RC-2 silane Figure 4(A) has two strong bands at 2974 cm⁻¹ and 959 cm⁻¹ due to the Si—OCH₃ group of the silane. The spectrum (after hydrolysis) in Figure 4(B) has two new bands at 3380 and 884 cm⁻¹ due
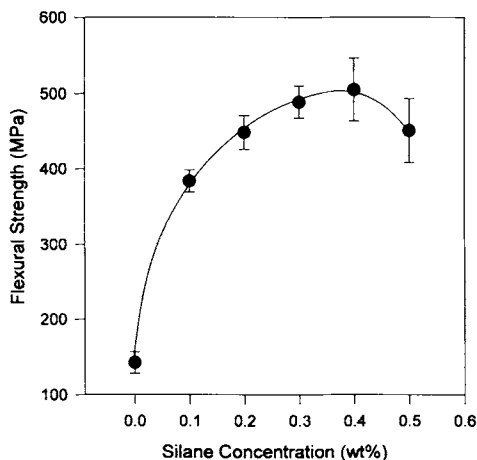

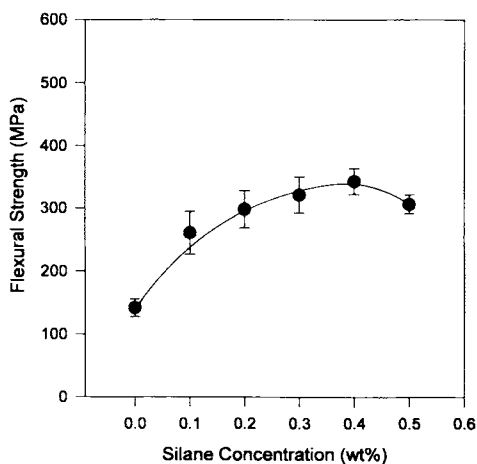**Figure 9** Flexural strength of RC-2 silane treated GF–PPS composite.

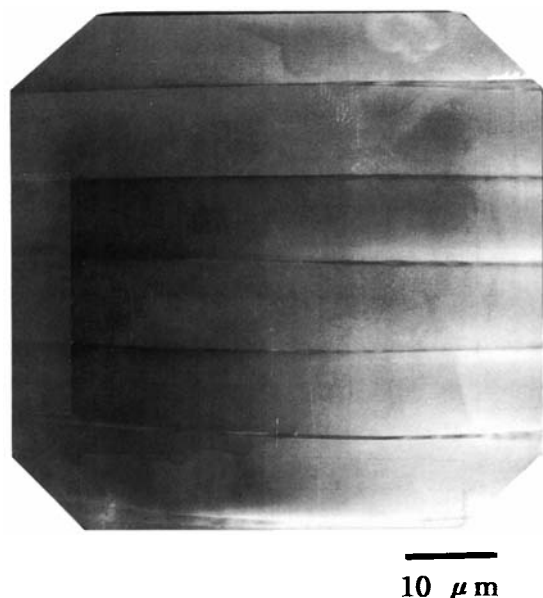**Figure 11** Flexural strength of styryl silane treated GF–PPS composite.

10 μ m

Figure 12 SEM micrograph of untreated GF–PPS composite.

to Si—OH group, but the bands at 2974 and 959 cm^{-1} disappear. From the above spectral data, it can be concluded that RC-2 silane is hydrolyzed efficiently under this experimental condition.

DRIFT spectrum of the RC-2 silane adsorbed onto the glass fiber surface is shown in Figure 5. Figure 5(A) is the spectrum of RC-2 silane treated glass fiber. Figure 5(B) is the spectrum of glass fiber, and the difference spectrum of (A) and (B) is shown in Figure 5(C). In Figure 5(C), the band at 3330 cm^{-1} due to the Si—OH group of RC-2 silane and the band at 2926 cm^{-1} due to the C—H stretching mode are observed. The presence of the band at 1594 cm^{-1} indicates that RC-2 silane has an aryl C—C bond. The band at 1187 cm^{-1} appears due to the Si—O—Si group from the condensation of RC-2 silanes. From these results, the RC-2 silane adsorbed onto the glass fiber surface can be identified.

Table I Basic Properties of Polyphenylene Sulfide

Property	PPS
Bulk density (g/cm^3)	0.30
Molecular weight (M_n)	30,000
Melting temperature (°C)	280

SUNTRA S 500 is the specific PPS analyzed.

Table II Basic Properties of Glass Fiber

Property	Glass Fiber
Specific gravity	2.54
Tensile strength at 22°C (MPa)	3448
Tensile modulus at 22°C (GPa)	72.4
Filament diameter (μm)	10

H-118 is the specific glass fiber analyzed.

Figure 6 shows the FT-IR transmittance spectra of styryl silane before and after hydrolysis. In Figure 6(A), the band at 3337 cm^{-1} is assigned to the N—H stretching mode. The bands at 2832, 1193, and 1030 cm^{-1} are due to Si—OCH$_3$ functional group of styryl silane. In Figure 6(B), the band due to Si—OH group of styryl silane is overlapped around 3421 cm^{-1} with the band due to the N—H bond of the silane. The band at 1581 cm^{-1} is assigned to the protonated —NH$_2^+$— group, and the band at 908 cm^{-1} is due to the Si—OH group of styryl silane after hydrolysis. From the above spectral assignments, it is ascertained that the styryl silane is efficiently hydrolyzed. Styryl silane after hydrolysis has a complex spectrum that is different from that of styryl silane only, especially around 2800–2400 cm^{-1} region and 1600–1400 cm^{-1} region. It was reported that these peculiar peaks appear because the amine-functional silane reacts with carbonic acid dissolved in water and forms protonated amine bicarbonate salts.[25]

Figure 7 represents the DRIFT spectrum of styryl silane adsorbed onto the glass fiber surface. Figure 7(A) is the spectrum of styryl silane treated glass fiber. Figure 7(B) is the spectrum of glass fiber only, and Figure 7(C) is the difference spectrum of (A) and (B). In Figure 7(C), the band at 3574 cm^{-1} is assigned to the N—H stretching mode of the styryl silane, and the band at 3275 cm^{-1} is due to the Si—OH group of the styryl silane. The band due to the C—H stretching mode appears at 2934 cm^{-1}. The band due to aryl C—C bond appears at 1562 cm^{-1}, and the band at 1159 cm^{-1} is due to Si—O—Si group. From the above results, it is confirmed that styryl silane was efficiently introduced onto the glass fiber surface.

Figure 8 shows the interlaminar shear strength (ILSS) of RC-2 silane treated GF–PPS composite as a function of RC-2 silane concentration. The ILSS of the composite increases as the silane concentration increases up to 0.4 wt %. At 0.5 wt % silane concentration, the ILSS of the composite decreases slightly. As RC-2 silane concentration in-
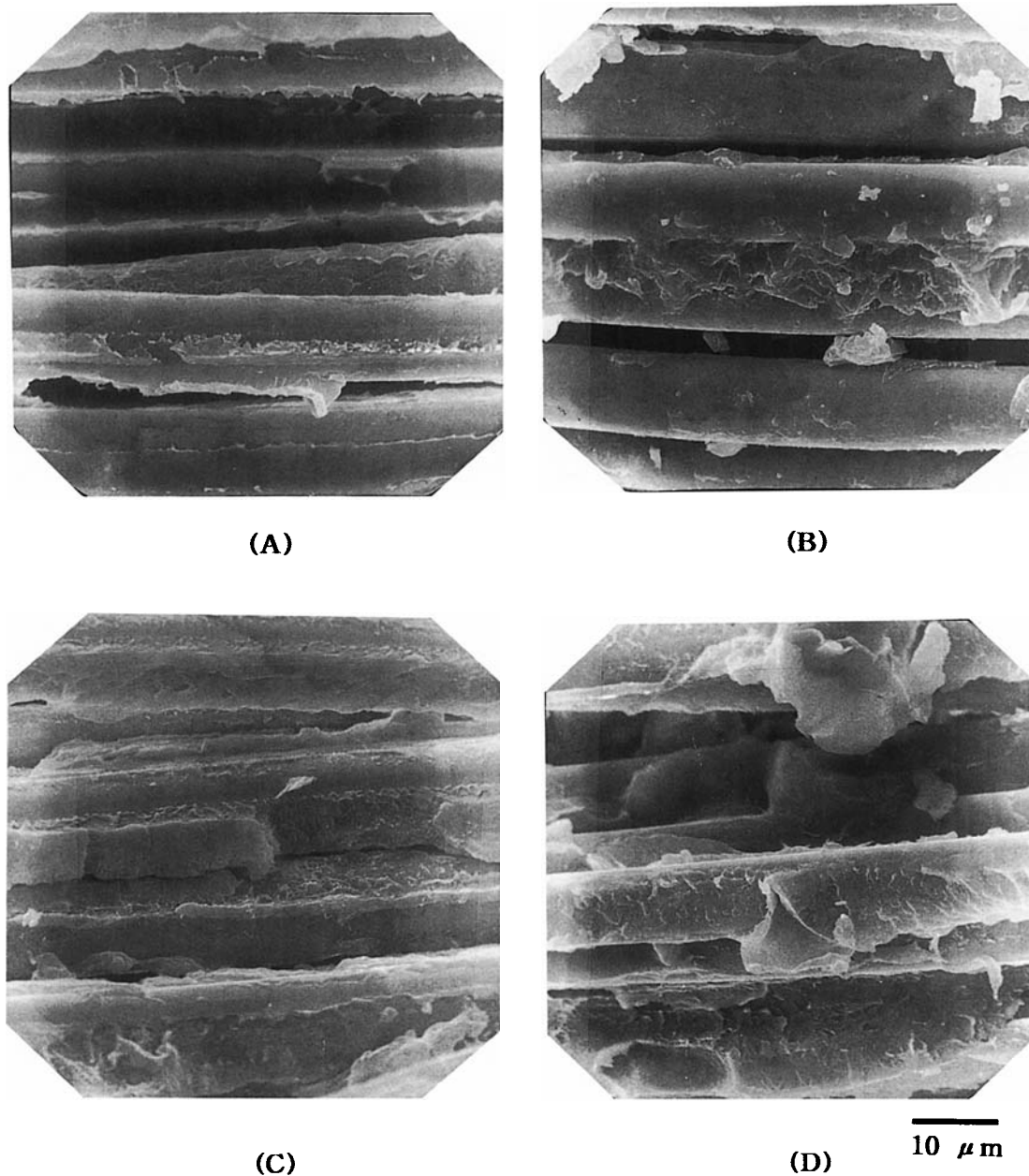
Figure 13   SEM micrographs of RC-2 silane-treated GF–PPS composite: (A) 0.1 wt %, (B) 0.2 wt %, (C) 0.3 wt %, (D) 0.4 wt %, and (E) 0.5 wt %.

creases, the amount of chemisorbed and physisorbed RC-2 silane, which can undergo chemical reaction with PPS or lead to the formation of IPN, increases. Therefore, the interfacial adhesion of the GF–PPS composite is improved by the RC-2 silane coupling agent through the chemical reaction or the IPN formation. The compatibility between the RC-2 silane and PPS is a minor factor in determining the interfacial strength of the composite since PPS is a crystalline polymer.[24] At 0.5 wt % silane concentra-

tion, the ILSS of the GF–PPS composite decreases due to the lubrication effect of the excess RC-2 silane coupling agent. When the excess silane is introduced onto the glass surface, a weak boundary layer is formed between the glass fiber and PPS, and it acts as a lubricant under the load.[24,26,27]

The flexural strengths of the RC-2 silane treated GF–PPS composite as a function of RC-2 silane concentration are shown in Figure 9. The flexural strength of the composite increases with increasing
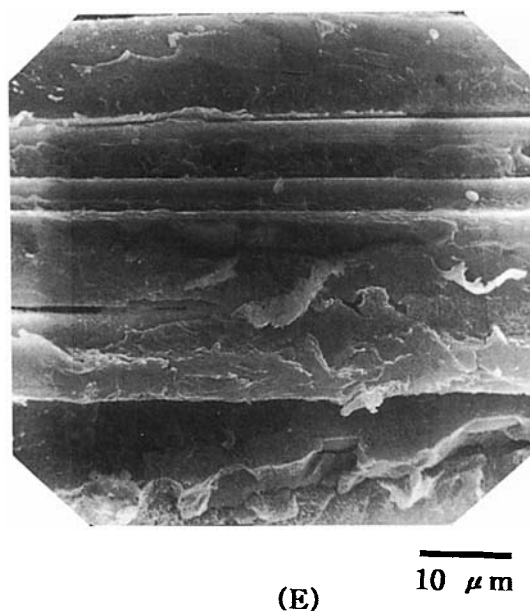
(E)　10 μm

Figure 13 (Continued from the previous page)

RC-2 silane concentration. The flexural strength of the composite shows a maximum value at 0.4 wt % silane concentration. The overall trend is similar to the case of the ILSS of the RC-2 silane-treated GF–PPS composite. From this similarity, it can be inferred that interfacial adhesion plays an important role in improving the mechanical properties of the GF–PPS composite.

Figure 10 indicates the ILSS of styryl silane treated GF–PPS composite as a function of styryl silane concentration. With increasing styryl silane concentration, the ILSS of the composite increases, and it gives the maximum value at 0.4 wt % silane concentration. The ILSS of the styryl silane treated GF–PPS composite decreases at 0.5 wt % silane concentration. This result can be explained in the same manner as the case of RC-2 silane treated GF–PPS composite. Excess silane adsorbed onto the glass fiber forms a weak boundary layer between glass fiber and PPS.

The ILSSs of styryl silane treated GF–PPS composites are smaller than those of RC-2 silane-treated ones. This is thought to be due to the effective IPN formation of RC-2 silane and the chemical interaction between RC-2 silane and PPS. First, it is possible that RC-2 silane has a structural advantage in making itself an efficient IPN. A RC-2 silane possesses three hydroxyl groups at each end after hydrolysis, whereas a styryl silane has three hydroxyl groups only at one end. Six directionally stretched

hydroxyl groups at both ends of RC-2 silane are thought to enable an IPN to be formed without geometric restrictions. In addition, a large number of hydroxyl groups in RC-2 silane can lead to a more dense network because of more siloxane bonds per molecule. Therefore, a three-dimensionally effective IPN structure can form more easily. Secondly, the polysulfide group of RC-2 silane has the possibility of participating in the crosslinking reaction of PPS, even though no clear evidence has been obtained. It is known that sulfur has been used for rubber vulcanization.[28]

Figure 11 shows the flexural strength of the styryl silane treated GF–PPS composite as a function of styryl silane concentration. The silane concentration is varied from 0.1–0.5 wt %. The overall trend is similar to the case of ILSS of the styryl silane treated GF–PPS composite. The flexural strength of the composite reaches the maximum value at 0.4 wt % silane concentration and then declines. This similarity implies that the interfacial adhesion of the composite is deeply related to the flexural strength of the composite. The flexural strengths of the styryl silane treated GF–PPS composites are smaller than those of the RC-2 silane treated ones.

SEM was used to investigate the morphological change of the fracture surface of the composite with various silane concentrations.

Figure 12 indicates the SEM microphotograph of the fracture surface of untreated GF–PPS composite. The untreated fiber surface is rarely coated with polymer. This fact shows poor adhesion at the GF–PPS interface. The glass fiber surface is inherently hydrophilic, but PPS is hydrophobic. Therefore, the glass fiber has low compatibility with PPS at the interface of the composite.

Figure 13(A–D) shows the SEM microphotographs of the fracture surfaces of RC-2 silane treated GF–PPS composites at various silane concentrations. As silane concentration increases [see Fig. 13(A–D)], the amount of entwined polymers onto the glass fiber surface increases. This demonstrates that the interfacial adhesion of the GF–PPS composite is improved compared with the untreated system. Figure 13(E) shows that the glass fiber is coated with less polymer than that in Figure 13(D). Excess silane gives rise to the poor adhesion between the glass fiber and PPS. This result coincides with the ILSS and the flexural strength data.

In Figure 14, the SEM microphotographs of the fracture surfaces of styryl silane treated GF–PPS composites are shown at various silane concentrations. As the styryl silane concentration increases
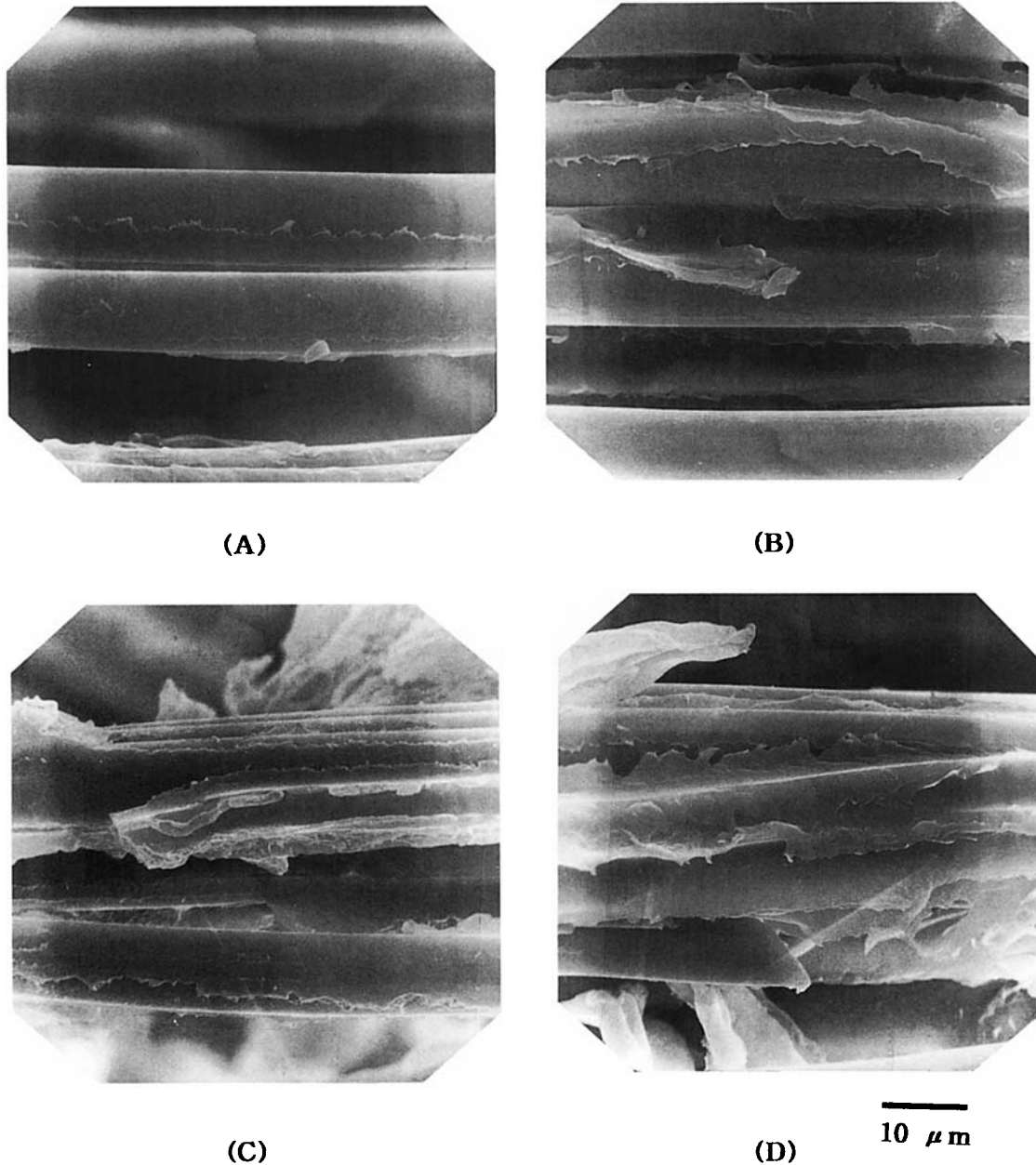
(A)

(B)

(C)

(D)

10 μ m

Figure 14   SEM micrographs of styryl silane treated GF–PPS composite: (A) 0.1 wt %,
(B) 0.2 wt %, (C) 0.3 wt %, (D) 0.4 wt %, and (E) 0.5 wt %.

up to 0.4 wt %, the polymer that sticks to the glass fiber surface becomes thicker. This means that the strength of the interfacial adhesion between glass fiber and PPS increases with increasing styryl silane concentration. At 0.5 wt % silane concentration, the glass fiber has smaller polymer coating on its surface than that at 0.4 wt %, which demonstrates that the interfacial adhesion strength between glass fiber and PPS decreases.

CONCLUSION

When glass fiber was treated with RC-2 and styryl silane adhesion promoters, the interlaminar shear stress and the flexural strength of GF–PPS composite increased. RC-2 silane was more efficient in enhancing the ILSS and the flexural strength of the GF–PPS composite. The optimum silane concentration for the improvement of the mechanical
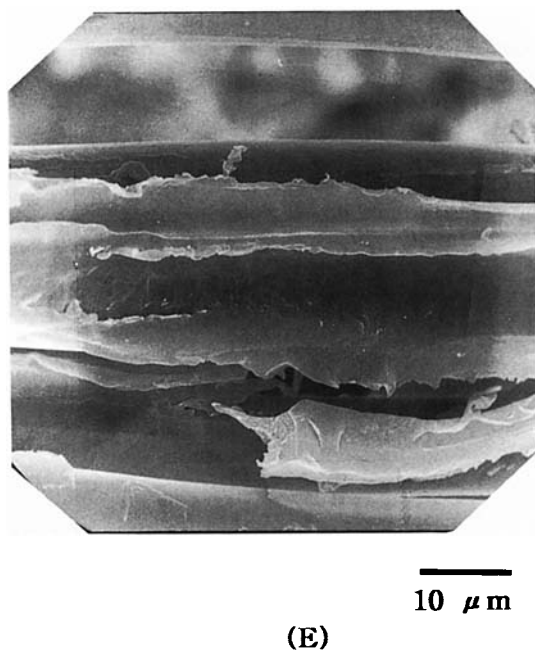
10 μm

(E)

Figure 14   (*Continued from the previous page*)

properties of the GF–PPS composite was 0.4 wt % in both cases of RC-2 and styryl silane. Because the ILSS and the flexural strength of the GF–PPS composite changed in a similar fashion as a function of silane concentration, it could be concluded that improved interfacial adhesion of the composite played an important role in strengthening the mechanical properties of the GF–PPS composite. From the SEM results, it was ascertained that the interfacial adhesion of the GF–PPS composite was efficiently improved when silane coupling agents were used.

REFERENCES

1. A. B. Strong, *Fundamentals of Composites Manufacturing: Materials, Methods, and Applications,* SME, Dearborn, 1989.
2. P. K. Mallick, *Fiber-reinforced Composites: Materials, Manufacturing, and Design,* Marcel Dekker, Inc., New York, 1988.
3. F. N. Cogswell, *Thermoplastic Aromatic Polymer Composite,* Butterworth-Heinemann, London, 1992.
4. L. A. Carlsson, *Thermoplastic Composite Materials,* Elsevier Science Publishers, New York, 1991.
5. J. J. Scobbo, Jr., *J. Appl. Polym. Sci.,* **47,** 2169 (1993).
6. L. Rebenfeld, G. P. Desio, and J. C. Wu, *J. Appl. Polym. Sci.,* **42,** 801 (1991).
7. K. C. Cole, D. Noël, and J. J. Hechler, *J. Appl. Polym. Sci.,* **39,** 1887 (1990).
8. J. Karger-Kocsis and K. Friedrich, *J. Mat. Sci.,* **22,** 947 (1987).
9. A. Kaul and K. Udipi, *Macromolecules,* **22,** 1201 (1989).
10. L. Caramaro, B. Chabert, J. Chauchard, and T. VU-Khanh, *Polym. Eng. Sci.,* **31**(17), 1279 (1991).
11. J. D. Menczel and G. L. Collins, *Polym. Eng. Sci.,* **32**(17), 1264 (1992).
12. M. W. Judek, B. Perkowska, and B. Karska, *J. Mat. Sci. Lett.,* **12,** 433 (1993).
13. H. Ishida and J. L. Koenig, *Polym. Eng. Sci.,* **18**(2), 128 (1978).
14. J. B. Donnet and G. Guilpain, *Carbon,* **27**(5), 749 (1989).
15. N. Menon, F. D. Blum, and L. R. Dharani, *J. Appl. Polym. Sci.,* **54,** 113 (1994).
16. L. Y. Yuan, S. S. Shyu, and J. Y. Lai, *J. Appl. Polym. Sci.,* **42,** 2525 (1991).
17. C. D. Han, C. Sandford, and H. J. Yoo, *Polym. Eng. Sci.,* **18**(11), 849 (1978).
18. L. J. Broutman, 25th Ann. Tech. Conf. Reinforced Plastics/Composites Div., SPI, Inc., Washington, D.C., 1970.
19. H. Ishida and K. Nakada, 42nd Ann. Tech. Conf. Composites Inst., SPI, Inc., Cincinnati, Feb. 2–6, 1987.
20. J. L. Koenig and H. Emadipour, *Pol. Compos.,* **6**(3), 142 (1985).
21. E. P. Plueddemann, 39th Ann. Tech. Conf. Reinforced Plastics/Composites Inst., SPI, Inc., Atlanta, Jan. 16–19, 1984.
22. E. P. Plueddemann and G. L. Stark, 35th Ann. Tech. Conf. Reinforced Plastics/Composites Inst., SPI, Inc., Boston, 1980.
23. H. Ishida and J. L. Koenig, *J. Colloid Interface Sci.,* **64**(3), 565 (1978).
24. E. P. Plueddemann, *Silane Coupling Agents,* Plenum Press, New York, 1982.
25. S. R. Culler, H. Ishida, and J. L. Koenig, *Pol. Compos.,* **7**(4), 231 (1986).
26. J. Jang, Ph.D. Diss., Case Western Reserve Univ., Cleveland, OH, (1988).
27. C. R. Choe and J. Jang, *Polymer (Korea),* **17**(6), 703 (1993).
28. C. M. Blow and C. Hepburn, *Rubber Technology and Manufacture,* Butterworth Scientific, London, 1982.